Scientific paper

Photodegradation of Adsorbed Bovine Serum Albumin on TiO_2 Anatase Investigated by In-Situ ATR-IR Spectroscopy

Ahmed Bouhekka[1,2,3] and Thomas Bürgi[1,*]

[1] *Département de Chimie Physique, 30 Quai Ernest-Ansermet, CH-1211 Genève 4, Switzerland*

[2] *Laboratoire de Physique des Couches Minces et Matériaux pour l'Electronique, Université d'Oran Es-Senia, 31100 Oran, Algeria*

[3] *Département de Physique, Université Hassiba Ben Bouali, 02000 Chlef, Algeria*

* *Corresponding author: E-mail: Thomas.Buergi@unige.ch*

Received: 20-03-2012

Abstract

A Fourier transform infrared-attenuated total reflection (FTIR-ATR) spectroscopy study of the photodegradation of adsorbed bovine Serum Albumin (BSA) on porous TiO_2 films was carried out. The experiments were performed in a flow-through cell in water at concentrations of 10^{-6} mol/L at room temperature. The curve fitting method of the second derivative spectra allowed us to explore details of the secondary structure of pure BSA in water and conformation changes during adsorption and illumination processes. The results clearly demonstrate that the amount of adsorbed BSA decreased under UV illumination although adsorption without illumination is considered as irreversible. The influence of irradiation on the adsorption is not yet well understood. Also, during illumination of adsorbed BSA dissolved CO_2 at 2341 cm^{-1} was observed, which indicates that part of the BSA is mineralized. The analysis of second derivative of infrared spectra was used to obtain direct quantitative information on the secondary structure components of BSA which show that the percentage of α-helix decreases from around 63% to 54% during UV light illumination whereas the percentage of β-turn increases.

Keywords: ATR-IR; TiO_2; Spin Coating; BSA; Protein Adsorption; Photocatalysis

1. Introduction

The transparent conductive oxides (TCO), such as TiO_2, SiO_2, and Al_2O_3, are used in many applications in such diverse areas as pigments, sunscreens, food colorants, wastewater treatment reactors, semiconductors, electrical insulators, and biomedical treatment.[1,2] Especially titanium dioxide (TiO_2), which exists in multiple structures such as: rutile, anatase and brookite[3], is an important material both for medical applications and as photocatalyst.

TiO_2 has big advantages for industrial photocatalysis compared to other materials. This is because TiO_2 combines high photoactivity and stability with lowest cost. This material has been used as a white pigment from ancient times because its safety to humans and environment is guaranteed by history.[4] Many studies have been published on the use of TiO_2 as a photocatalyst for the decomposition of organic compounds. TiO_2 has a gap around 3 eV, so it is active under ultraviolet light (UV) irradiation, and creates electron hole pairs as a result of absorbing UV light.[5–7] Upon UV light illumination photochemical reactions take place on a TiO_2 surface such as photo-induced redox reactions of adsorbed molecules, and the photo-induced hydrophilic conversion of TiO_2.[4]

The TiO_2 water interface is also important in a number of disciplines like biology, biotechnology, biochemical engineering, medicine and environment sciences. It is therefore very important to understand protein adsorption, a very complex process driven by different protein-surface forces, from an aqueous environment to TiO_2. Protein adsorption on a solid surface may induce changes in their structures and functions.[8,9] There are several important research questions which are not yet well answered like the

conditions under which proteins adsorb, the parameters that control the adsorption process, whether the proteins are still bioactive or not when they get adsorbed to a surface and especially how do adsorbed proteins onto semiconductor surface behave under irradiation?

Here we study the interaction of bovine serum albumin (BSA) with TiO_2 and its behavior under photocatalytic conditions, i.e. under UV irradiation by using in situ attenuated total reflection (ATR) infrared spectroscopy. BSA was selected as it is stable, available at high purity, soluble in water and it can be attached to different surfaces. BSA is widely used as a model protein and according to literature[10–16] it has a molecular mass between 66 kDa and 68 kDa and is built from 583–607 amino acids linked together by peptide bonds. The secondary structure of BSA is composed of ~67% α-helix, ~10% turn, and around 23% extended chain and no β-sheet is contained. It is shown that part of the protein is mineralized and that the irradiation leads to significant changes in the relative amount of secondary structure elements.

2. Experimental

2. 1. TiO_2 Thin Film Preparation

Commercial type TiO_2 anatase (Sigma-Aldrich Chemie GmbH) with an average particle size less than 25 nm (specific surface area 200–220 m^2/g, density: 3.9 g/mL at 25 °C) was used in the photocatalytic experiments. The catalyst films were prepared by suspending 20 mg of TiO_2 anatase in 10 ml of purified water (Milli-Q, Millipore) water (18 MΩ cm). The slurry was sonicated for 30 min. The film was formed by dropping the slurry onto a Ge internal reflection element (IRE, 52 mm × 20 mm × 1 mm, Komlas GmbH). Before film deposition the IRE was first cleaned with ethanol and then put in air plasma for around 15 min. The solvent was evaporated using the spin coating method (1000 rotation per minute) twelve successive spin coatings were applied with 2.25 minutes between the individual coating steps. Then the samples were dried at 80 °C for some hours in an oven. After drying the film was ready for use. For every experiment a fresh catalyst film was prepared, and results were reproducible on different catalyst films. Bovine serum albumin (BSA, Sigma-Aldrich) (68 kDa, solubility 1g in 25 ml of H_2O) was used to prepare a BSA solution of 10^{-6} mol/L in all experiments. The pH of the solution was about 5.4, which is between the isoelectric points of BSA (4.8) and TiO_2 (6.4).

2. 2. Attenuated Total Reflection Infrared Spectroscopy

Attenuated total reflection infrared (ATR-IR) spectroscopy is a well established experimental technique to investigate processes taking place at solid-liquid interfaces.[17–21] ATR spectra were recorded with a dedicated flow-through cell, made from a Teflon piece, a fused silica plate (45 mm × 35 mm × 3 mm) with holes for the inlet and outlet (36 mm apart), and a flat (1 mm) viton seal. The cell was mounted on an attachment for ATR measurements within the sample compartment of a Bruker Equinox 55 FTIR spectrometer equipped with a narrow-band MCT detector. Spectra were recorded at a room temperature at a resolution of 4 cm^{-1}.

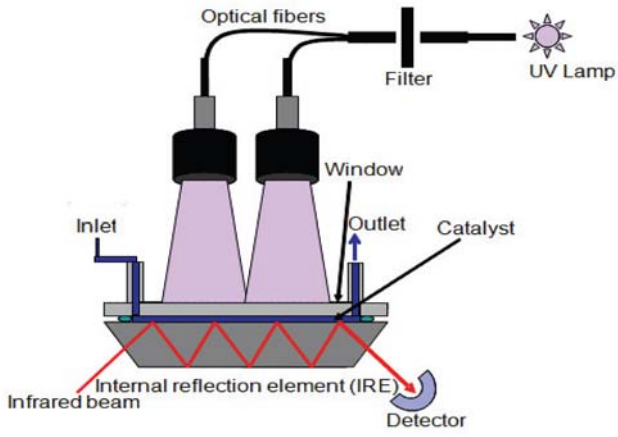

Figure 1. Schematic of the experimental setup for in situ ATR-IR spectroscopy and UV-light irradiation for the investigation of photocatalytic reactions taking place at solid-liquid interfaces. Adapted with permission from.[5] Copyright Elsevier (2007).

The aqueous BSA solution can pass through the cell and over the sample by means of peristaltic Pump (Ismatec, Reglo 100) located after the cell. A constant flow rate of about 0.2 ml/min was used.

In ATR-IR, a beam of infrared light is passed through the ATR crystal (Ge) as shown in Figure 1, in such a way that it reflects at least once off the internal surface in contact with the sample. This reflection leads to an evanescent field which extends into the sample. The penetration depth into the sample is typically between 0.5 and 2 micrometers, with the exact value being determined by the wavelength of light, the angle of incidence and the indices of refraction of the ATR crystal and the medium being probed. The beam is then collected and guided to a detector as it exits the crystal. Illumination of the sample with UV light was carried out using a 75 W Xe arc lamp. The UV light from the source is guided to the cell via two fiber bundles. The light was passed through a 5 cm water filter to remove any infrared radiation. A Schott UG 11 (50 × mm × 50 mm × 1 mm) broadband filter from ITOS was used to remove visible light (transmission between 270 and 380 nm). The intensity of the UV light at the surface is measured to be 2–4 mw/cm^2 and the temperature is increased by around 2 °C.

2. 2. 1. ATR-IR of Proteins

Although water (H_2O) is challenging for IR spectroscopy, it is much preferable over D_2O for studying protein structure because it has the advantage of providing a more native environment.[22–26] D_2O changes the protein properties somewhat with respect to the native state because the amide I bands are strongly affected by the H-D exchanges in the peptide linkages.[27–30] In H_2O solution, the bands between 1654 cm^{-1} and 1658 cm^{-1} are assigned to α-helix. The unordered conformation (random coil) is usually associated with the IR band between 1640 cm^{-1} and 1648 cm^{-1}, beta turn is found between 1675 cm^{-1} and 1685 cm^{-1}, β-sheet absorbs from 1690 cm^{-1} to 1696 cm^{-1} and from 1624 cm^{-1} to 1642 cm^{-1}, and intermolecular β-sheet gives rise to a signal around 1615 cm^{-1}.[22]

The correction of the spectra from water absorption is always a concern. H_2O has a strong IR absorbance around 3400 cm^{-1} (O-H stretching), 2125 cm^{-1} (water association combination band) and 1640 cm^{-1} (H-O-H bending). The amide I mode of proteins absorbs between 1600 cm^{-1} and 1700 cm^{-1}, overlapping directly with the H_2O bending vibrational mode at 1640 cm^{-1}.[22] For ATR-IR study of proteins in H_2O solution, water absorption in the region 1600–1700 cm^{-1} is the biggest problem whereas D_2O has no absorption band in the spectral region of the amide I and amide II bands.[22]

The contribution of water in the protein spectrum can be eliminated using digital subtraction by measuring water and the protein in water at identical conditions. There are two criteria that allow a good subtraction of absorption bands due to liquid water and gaseous water in the atmosphere. First, the sharp bands originating from water vapor must be subtracted accurately from the protein spectrum between 1800 and 1500 cm^{-1}. Second, a straight baseline must be obtained from 2000 to 1750 cm^{-1}. Using these two criteria to judge the successfulness of water subtraction leads to a higher quality of protein spectra.[23,31–34] The validity of this approach was tested by determining the content of the secondary structure elements of dissolved BSA in water using ATR-IR and a curve fitting of the second derivative spectra (see later). Using this procedure the known composition of secondary structure elements of dissolved BSA could be well reproduced.

3. Results and Discussion

The spectrum of adsorbed BSA on the surface of TiO_2 under equilibrium conditions is shown in Figure 2. No corrections were made for water compensation. The negative water bands around 1640 and 3000–3700 cm^{-1} are due to displacement of water molecules from the interface due to protein adsorption.

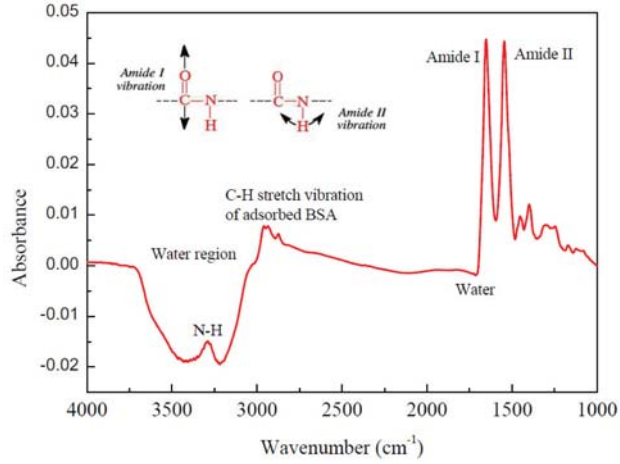

Figure 2. ATR-IR spectrum of BSA on TiO_2 close to equilibrium situation and peaks identification. No corrections were made.

3. 1. Adsorption of BSA on TiO_2 and Effect of UV Illumination

Figure 3 shows the evolution of ATR spectra of BSA adsorbed on TiO_2 as a function of time as the system evolves towards the equilibrium and Figure 4 shows the effect of UV light. Before illumination BSA was adsorbed for about 80 minutes. It is clear that UV light decreases the amount of adsorbed BSA. It is well known that the band gap of TiO_2 anatase is about 3 eV. UV light illumination leads to the creation of electron hole pairs that can migrate to the surface of the TiO_2 and react with adsorbed BSA. This phenomenon is complex and still not very well understood right now.

Figure 5 shows the signal at 1654 cm^{-1} as a function of time for BSA adsorbed on TiO_2 followed by rinsing by water and UV illumination. The adsorption is initially

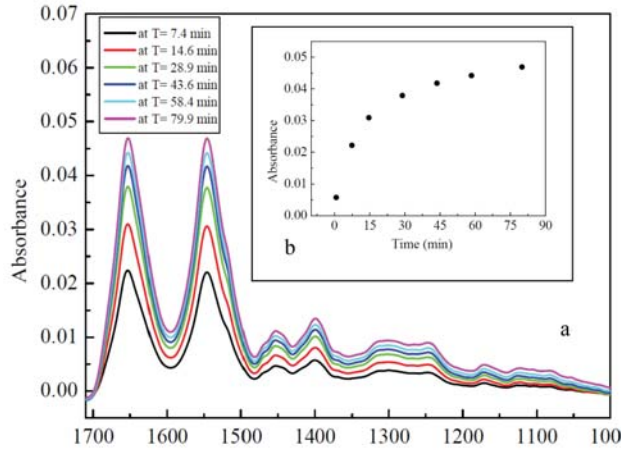

Figure 3. ATR-IR spectra recorded during adsorption of BSA onto TiO_2. Equilibrium was reached after about 80 minutes. a) Absorbance spectra collected in situ, b) variation of amide I band versus time.

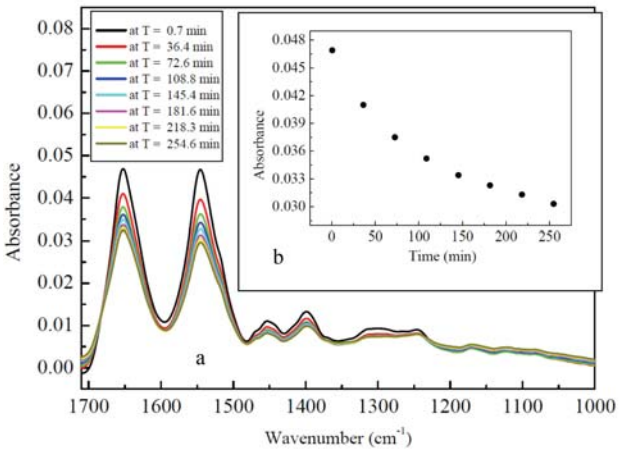

Figure 4. The effect of UV light on the adsorbed BSA. a) Absorbance spectra collected in situ (spectra were collected while flowing water and illuminating with UV light), b) variation of amide I band versus time.

very fast but slows down with time as the surface gets crowded. Upon flowing water the signal remains constant, indicating that BSA remains adsorbed under these conditions. By UV illumination one part of the BSA is removed but the removal seems to stabilize at some point, indicating that some of the BSA molecules are "irreversibly" bound to the surface. This behavior is still not well understood and it could be caused by the changes of the surface properties during elongated UV illumination. According to literature, the photocatalytic activity of TiO_2 has been found to be tied to the surface properties of the catalyst. Some of the particle properties which are known to affect the photocatalytic activity are particle size, crystal structure, amounts and the identity of defects and preparation method.[35–38] It has been found that UV irradiation of the titanium dioxide surface will induce superhydrophilicity, which changes the nature of a surface from hydrophobic to hydrophilic by removing organic compounds, inducing oxygen vacancies and breaking Ti-O-Ti and O-H bonds at the surface.[39–44]

We have seen also the appearance of a peak at 2341 cm^{-1} (Figure 6) characteristic of dissolved CO_2. This is a strong indication that mineralization of BSA takes place upon illumination of the surface by UV (light).

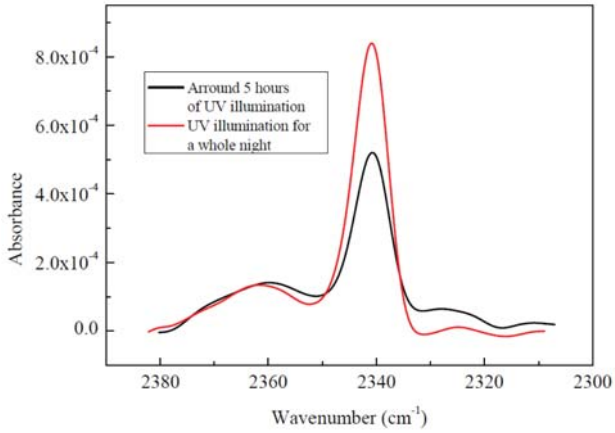

Figure 6. The appearance of a peak at 2341 cm^{-1} after UV illumination for 5 hours and during the whole night. Spectra were smoothed using smooth function (Savitzky-Golay algorithm) in OPUS program to omit the noise.

In order to get some more information on the nature of the desorbing species upon irradiation of adsorbed BSA we used UV-vis spectroscopy (Jasco 650). Figure 7 shows the absorption spectrum of pure BSA in water (10^{-6} mol/L). The two peaks around 280 nm (less intense) and around 210 nm (more intense) are due the aromatic groups and amide groups, respectively, in BSA.

A pure solution of BSA in water was irradiated by UV light for more than two hours and after that the meas-

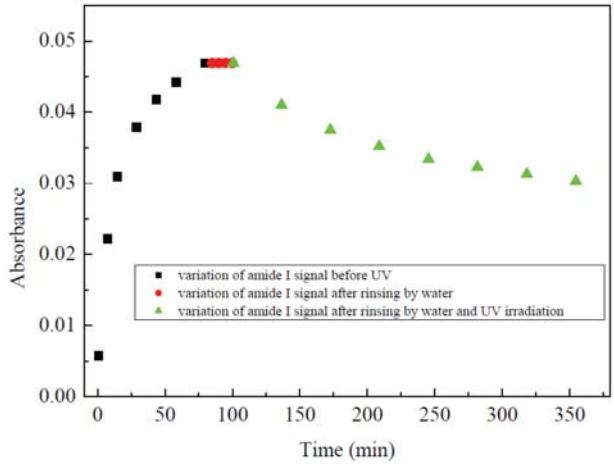

Figure 5. Absorbance at 1654 cm^{-1} corresponding to the amide I band of BSA adsorbed on TiO_2 as a function of time during adsorption, rinsing by water and UV illumination.

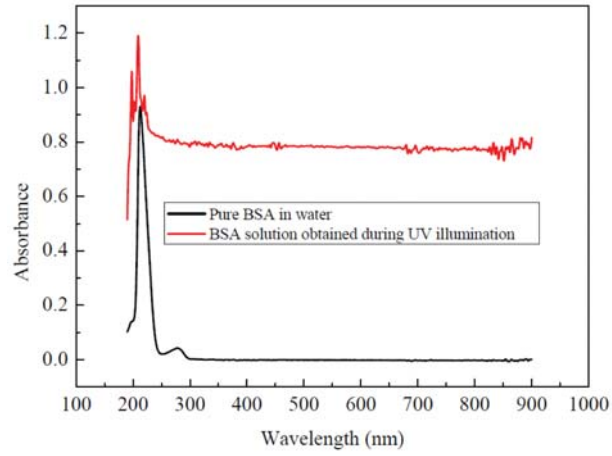

Figure 7. Absorbance of pure BSA in water at a concentration of 10^{-6} mol/l and solution obtained during illumination of adsorbed BSA by UV multiplied 10 times.

ured UV-vis spectrum did not show any changes with respect to the one measured before irradiation.

As it is evident from the ATR experiments that part of the adsorbed BSA is removed from the TiO_2 surface upon irradiation we have collected the cell effluent during such an experiment and the collected solution was analyzed by UV-vis spectroscopy (Figure 7). It is evident that the spectrum is different from the one of BSA in solution.

The observations confirm that the UV light does not desorb the whole protein from the surface of TiO_2 but it may cut it into smaller pieces, as it is expected by other authors.[6] At least one part is even completely mineralized thus leading to the formation of CO_2. Interestingly, the removal of BSA from the surface becomes very slow after some time.

To study the effect of adsorption and of UV irradiation on the secondary structure of BSA we determined the percentage of secondary structure elements of BSA by analysis of the second derivative of the amide I band. For comparison we measured the ATR spectrum of the protein dissolved in water. For this we prepared a solution of high concentration of BSA ($2*10^{-4}$ mol/L). The ATR spectra

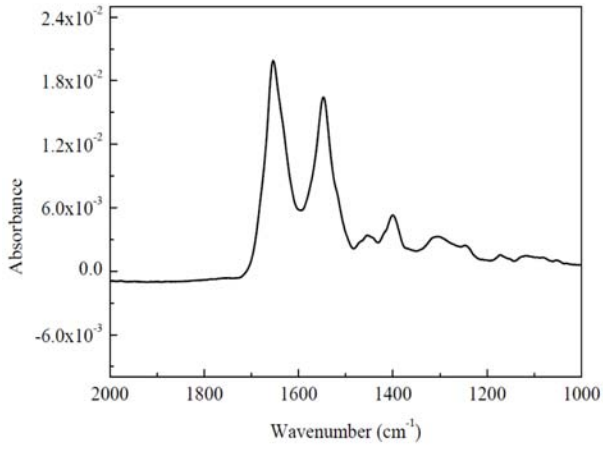

Figure 8. Corrected spectrum of pure BSA in solution at a concentration of $2*10^{-4}$ mol/L from water using the two criteria.

were then measured while flowing the BSA solution over a clean Ge internal reflection element. After rinsing with pure water another spectrum was recorded. The latter spectrum was subtracted from the spectrum recorded while flowing the BSA solution. This procedure ensures that BSA adsorbed on the internal reflection element is not considered. The resulting solution spectrum is corrected from water using the two criteria mentioned above and the final spectrum is shown in Figure 8.

Figure 9 shows the negative second derivative of the amide I region and the result of the curve fitting procedure which yields the following contributions of secondary structure elements for BSA in solution: Intermolecular β-sheet at 1613.8 cm^{-1}: 1.5%; β-sheet (or β-strands, short

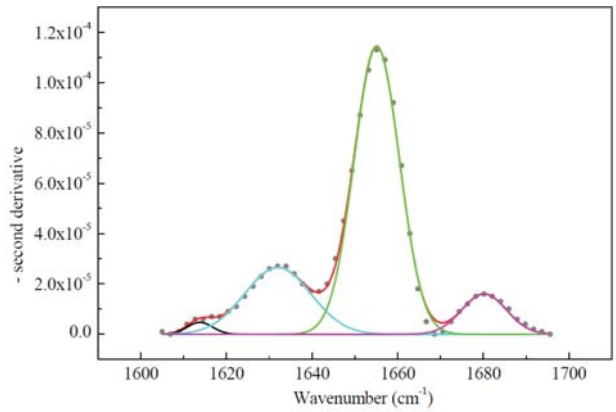

Figure 9. Curve fitting of negative second derivative of pure BSA in water solution at concentration of $2*10^{-4}$ mol/L.

segments connecting helical structures[10,45]) at 1632.0 cm^{-1}: 22.5%; α-helix at 1655.1 cm^{-1}: 66.6%; turn at 1680.2 cm^{-1}: 9.2%. These percentages are in good agreement with the literature.[10–16]

The same procedure is applied to study the secondary structure of BSA during adsorption (Table 1) and under UV irradiation (Table 2). The table 1 shows the result of negative second derivative fitting of adsorbed BSA on TiO_2 before UV irradiation.

Table 1. Curve fitting results of negative second derivative of adsorbed BSA on TiO_2 before UV irradiation (% is the percentage corresponds to each peak at different times).

Time min → **Peak ↓**	**7.4**	**14.6**	**28.9**	**43.6**	**58.4**	**79.9**
1614 cm^{-1} → %	1.5	2.0	1.7	2.2	2.2	2.5
1634 cm^{-1} → %	25.5	24.5	25.1	24.3	24.7	24.9
1655 cm^{-1} → %	64.1	63.5	62.7	63.9	63.1	62.5
1680 cm^{-1} → %	8.7	9.8	10.3	9.6	9.9	10.0

According to table 1, the percentages of the secondary structure elements are quite stable during adsorption with a slight decrease of α-helix at higher coverage. During UV irradiation (Table 2) however the percentage of α-helix decreases clearly.

This behavior is graphically represented in figure 10 which shows the decrease of α-helix from around 62 % before UV irradiation to around 54 % and the increase of beta turn from around 10 % to 16 % after UV illumination, respectively.

This behavior can be explained by the transformation of α-helix structure to β-turn during the photodegradation of adsorbed BSA on TiO_2. As discussed above, UV irradiation does not remove the whole protein from the surface but it might cut it into smaller pieces. The main effected secondary structure in the adsorbed BSA is α-helix

Table 2. Curve fitting results of negative second derivative of adsorbed BSA on TiO_2 after UV irradiation (% is the percentage corresponds to each peak at different times).

Time min → **Peak ↓**	**0.7**	**36.4**	**72.6**	**108.8**	**145.4**	**181.6**	**218.3**	**254.6**
1614 cm^{-1} → %	2.0	2.4	2.2	1.8	1.5	2.0	2.0	2.4
1634 cm^{-1} → %	25.1	24.2	26.1	26.1	26.6	26.6	27.1	26.7
1654 cm^{-1} → %	62.5	60.2	58.1	57.3	56.7	55.8	54.7	54.0
1680 cm^{-1} → %	10.4	12.8	13.3	14.7	15.1	15.5	16.0	16.5

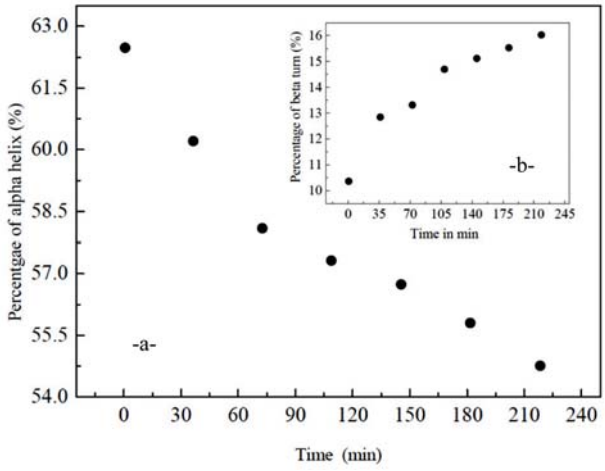

Figure 10. Variation of the percentage of: a) α-helix and b) β-turn during UV illumination.

(that represents also the major fraction with about 65 %). The damage made to the protein during photocatalysis seems to destabilize the α-helix structure. Note that the changes in the secondary structure of adsorbed BSA observed during UV irradiation are different from the ones observed by heating the sample. In the latter case the analysis of the amide I bands points towards the formation of random coil structure (results are not shown here) in agreements with earlier reports.[45,10]

4. Conclusion

ATR-IR spectroscopy and spectrophotometry were used to study the photodegradation of BSA over porous thin films of TiO_2 anatase prepared by spin coating technique. Our results under shining the adsorbed BSA on TiO_2 with UV light clearly show reducing the amount of BSA exists on the surface which is considered as irreversible after rinsing with purified water. We have furthermore seen that UV illumination does not desorb the whole protein from the TiO_2 surface but it might cut it into small pieces. The most likely explanation of the appearance of the peak at 2341 cm^{-1} corresponds to dissolved CO_2 in water is that one of the final products of the photodegradation process is CO_2. The curve fitting of second derivative of amide I band, after correcting spectra from liquid and vapor water, permits direct quantitative analysis of the secondary structural components of adsorbed BSA and clearly demonstrate the decrease of the percentage of α-helix under UV light illumination this behavior is totally different from the effect of pH and temperature.

5. Acknowledgment

Funding was provided by the University of Geneva in Switzerland and by DAAD at the University of Heidelberg in Germany.

6. References

1. R. J. Aitken, M. Q. Chaudhry, A. B. A. Boxall, M. Hull *Occup. Med-Oxford* **2006**, *56(5)*, 300–306.
2. L. K. Adams, D. Y. Lyon, P. J. J. Alvarez, *Water Res.* **2006**, *40(19)*, 3527–3532.
3. M. Paine, J. Wong, Osteoblast Response to Pure Titanium and Titanium Alloy, in J. Ellingsen, S. Lyngstadaas (eds.), Bio-implant Interface. Improving Biomaterials and Tissue Reactions, CRC Press, **2003**.
4. K. Hashimoto, H. Ierie, A. Fujishima, *J. Appl. Phys.* **2005**, *44*, 8269–8285.
5. I. Dolamic, T. Bürgi, *J. Catal.* **2007**, *248*, 268–276.
6. I. Dolamic, T. Bürgi, *J. Phys. Chem. C* **2011**, *115*, 2228–2234.
7. L. Linsebigler, G. Lu, J. T. Yates, Jr, *Chem. Rev.* **1995**, *95,* 735–758
8. A. Bhaduri, K. P. Das, *J. Disper. Sci. Technol.* **1999**, *20(4)*, 1097–1123.
9. K. Nakanishi, T. Sakiyama, K. Imamura, *J. Biosci. Bioeng*. **2001**, *91(3)*, 233–244.
10. K. Murayama, M. Tomida, *Biochem.* **2004**, *43*, 11526–11532.
11. T. Peters, *J. Biochem. Genet. Medic. Appl*, Academic Press, San Diego **1996.**
12. D. C. Carter, J. X. Ho, *Adv. Protein Chem.* **1994**, *45*, 153–203.
13. J. R. Brown, Albumin: Structure, Function and Uses, in V. M. Rosenoer, M. Oraz, M. A. Rotshild (eds.), Pergamon Press, Oxford, **1977**.

14. Structure Explore-1AO6, Protein Data Bank, Department of Chemistry, Brookhaven National Laboratory, Upton, NY 11973, Database available at http://www.pdb.bnl.gov/index.html.
15. R. G. Reed, R. C. Feldhoff, O. L. Clute, T. Peters, *Biochem.* **1975**, *14*, 4578–4583.
16. R. Wetzel, M. Becler, J. Behlke, H. Billwitz, S. Bohm, B. Ebert, H. Haman, J. Krumbiegel, G. Lassmann, *Eur. J. Biochem.* **1980***, 104*, 469–478.
17. S. J. Hug, B. Sulzberger, *Langmuir* **1994**, *10(10)*, 3587–3597
18. A. Urakawa, R. Wirz, T. Burgi, A. Baiker, *J. Phys. Chem. B* **2003,** *107*, (47), 13061 13068.
19. T. Burgi, R. Wirz, A. Baiker, *J. Phys. Chem. B* **2003,** *107*, (28), 6774–6781.
20. T. Bürgi, A. Baiker., *Adv. Cataly.* **2006,** *50*, 227–283.
21. R. P. Sperline, Y. Song, H. Freiser, *Langmuir* **1992,** *8*, 2183–2191.
22. J. Kong, S. Yu, *Acta Biochim. Biophys. Sinica* **2007**, *39(8)*, 549–559.
23. S. Y. Venyaminov, N. N. Kalnin, *Biopolym.* **1990**, *30*, 1243–1257.
24. S. Y. Venyaminov, N. N. Kalnin, *Biopolym.* **1990**, *30*, 1259–1271.
25. N. N. Kalnin, I. A. Baikalov, S. Y. Venyaminov, *Biopolym.* **1990**, *30*, 1273–1280
26. A. Dong, P. Huang, W. S. Caughey, *Biochem.* **1990**, *29*, 3303–3308.
27. P. Cioni, G. B. Strambini, *J. Biophys.* **2002**, *82*, 3246–3253.
28. G. I. Makhatadze, G. M. Clore, A. M. Gronenborn, *Nat. Struct. Biol.* **1995**, *2*, 852–855.
29. H. Susi, D. M. Byler, *Biochem. Biophys. Res. Comm.* **1983**, *115*, 391–397.
30. D. M. Byler, H. Susi, *Biopolym.* **1986**, *25*, 469–487.
31. A. Dong, P. Huang, W. S. Caughey, *Biochem.* **1992**, *31*, 182–189.
32. W. K. Surewicz, A. G. Szabo, H. H. Mantsch, *Eur. J. Biochem.* **1987**, *167*, 519–523.
33. R. C. Mitchell, P. I. Haris, C. Fallowfield, D. J. Keeling, D. Chapman, *Biochim. Biophys. Acta* **1988**, *94*, 31–38.
34. J. C. Gorgat, A. Dong, M. C. Manningt, R. W. Woodyf, W. S. Caugheyt, J. L. Strominger, *Proc. Nati. Acad. Sci. USA Immunology* **1989**, *86*, 2321–2325.
35. O. Carp, C. L. Huisman, A. Reller, *Prog. Solid. State. Chem.* **2004**, *32*, 33–177.
36. H. Jensen, K. D. Joensen, J. E. Jørgensen, J. S. Pedersen, E. G. Søgaard, *J. Nanoparticle Res* **2004**, *6*, 519–526.
37. M. Kang, S. Y. Lee, C. H. Chung, S. M. Cho, G. Y. Han, B. W. Kim, K.J. Yoon, *J. Photochem. Photobiol.* **2001**, *A 144*, 185–191.
38. J. Yu, J. Xiong, B. Cheng, S. Liu, *Appl. Catal. B: Environ.* **2005**, *60*, 211–221.
39. A. Fujishima, T. N. Rao, *Pure Appl. Chem.* **1998**, *70 (11),* 2177–2187.
40. N. Sakai, A. Fujishima, T. Watanabe, K. Hashimoto, *J. Phys. Chem. B* **2001**, *105*, 3023– 3026.
41. N. Sakai, A. Fujishima, T. Watanabe, K. Hashimoto, *J. Phys. Chem. B* **2003**, *107*, 1028– 1035.
42. J. M. White, J. Szanyi, M. A. Henderson, *J. Phys. Chem. B* **2003**,*107 (34)*, 9029–9033.
43. T. Zubkov, D. Stahl, T. Thompson, D. Panayotov, O. Diward, J. T. Yates, *J. Phys. Chem. B* **2005**, *109*, 15454–15462.
44. A. Mills, M. Crow, *J. Phys. Chem. C* **2007**, *111 (16)*, 6009–6016.
45. S. C. Wang, C. Ted Lee, *J. Phys. Chem. B* **2006**, *110*, 16117–16123.

Povzetek

Z infrardečo spektroskopijo na oslabljeni popolni odboj s Fourierjevo transformacijo (FTIR-ATR) smo izvedli študijo fotorazgradnje adsorbiranega govejega serumskega albumina (BSA) na poroznem TiO_2 filmu. Eksperiment smo izvedli v pretočni celici v vodnem okolju pri koncentracijah 10^{-6} mol/L in pri sobni temperaturi. Metoda prilagoditve krivulji za drugi odvod spektra je omogočila vpogled v sekundarno strukturo čistega BSA v vodi in opazovanje konformacijskih sprememb med adsorpcijo in procesom osvetljevanja. Rezultati jasno kažejo, da se pod vplivom UV osvetlitve količina adsorbiranega BSA zmanjša, medtem ko je količina adsorbiranega BSA brez osvetljevanja nespremenjena. Vpliv osvetlitve na adsorpcijo še ni dobro pojasnjen. Med osvetljevanjem smo v spektru adsorbiranega BSA opazili vrh za raztopljeni CO_2 pri 2341 cm^{-1}, kar nakazuje na delno mineralizacijo BSA. Z analizo drugega odvoda infrardečih spektrov smo pridobili direktne kvantitativne informacije o sekundarni strukturi komponent BSA, ki kažejo, da se z UV osvetljevanjem zniža delež α-vijačnic s približno 63 % na 54 %, medtem ko se delež β-zavojev poveča.